



CHORUS

This is the accepted manuscript made available via CHORUS. The article has been published as:

## Effect of Local Chain Conformation in Adsorbed Nanolayers on Confined Polymer Molecular Mobility

Biao Zuo, Hao Zhou, Mary J. B. Davis, Xinping Wang, and Rodney D. Priestley

Phys. Rev. Lett. **122**, 217801 — Published 29 May 2019

DOI: [10.1103/PhysRevLett.122.217801](https://doi.org/10.1103/PhysRevLett.122.217801)

# The Effect of Local Chain Conformation in Adsorbed Nanolayers on Confined Polymer Molecular Mobility

Biao Zuo,<sup>1,2</sup> Hao Zhou,<sup>1</sup> Mary J. B. Davis,<sup>2</sup> Xinping Wang<sup>1,\*</sup> and Rodney D. Priestley<sup>2,3,†</sup>

<sup>1</sup>Department of Chemistry, Zhejiang Sci-Tech University, Hangzhou 310018, China

<sup>2</sup>Department of Chemical and Biological Engineering, Princeton University, Princeton, New Jersey 08544, United States

<sup>3</sup>Princeton Institute for the Science and Technology of Materials, Princeton University, Princeton, New Jersey 08544, United States

## **Abstract**

Interfaces play an important role in modifying the dynamics of polymers confined to the nanoscale. Here, we demonstrate that the distance over which an interface suppresses molecular mobility in poly(styrene) thin films can be systematically increased by tens of nanometers by controlling the chain conformation, i.e., height of loops in irreversibly adsorbed nanolayers. These effects arise from topological interaction between adsorbed and neighboring un-adsorbed chains, respectively, which increase their motional coupling to facilitate the propagation of suppressed dynamics originating at the interface, thus highlighting the ability to manipulate interfacial effects by local conformation of chains in adsorbed nanolayers.

**Main Text** The dynamics of polymers confined to the nanoscale are different from those of the bulk. [1-8] Consensus is emerging that interfaces, which can alter the conformation of nearby chains, are the underpinnings of confinement effects on molecular dynamics. [2-5] Modified dynamics at the interface can propagate over a length scale of tens of nanometers, [6-8] creating a percolation network which alters average mobility [9,10]. Hence, understanding the pathway by which interfacial mobility propagates within confined polymers is of critical importance. Moreover, our ability to harness such effects, by systematically controlling the length scale over which modified dynamics propagate away from the interface, would provide a unique means to exploit confinement to tune polymer properties.

Irreversibly adsorbed nanolayers, immobilized ultrathin layers of polymers strongly adhered atop a solid surface, are worthy of special attention, because their structure and properties are crucial to how interfacial effects impact thin film dynamics. Napolitano et al. [11-14] demonstrated that substrate effects on the glass transition temperature ( $T_g$ ) and segmental dynamics, measured in thin films upon confinement, could be directly related to the degree of chain adsorption at the substrate. Koga et al. [15], Wang et al. [16-18] revealed that suppressed dynamics of ultrathin adsorbed layers could extend tens of nanometers away from the substrate, which could be related to the thickness or architecture of the adsorbed layer. Meanwhile, Burroughs et al. found that such layers have an enhanced  $T_g$  [19]. It has been proposed that adsorbed layer effects on molecular mobility are realized by topological interactions between structures within adsorbed chains, i.e., loops, and those of neighboring un-adsorbed chains in matrix, which ensure continuity in the mobility gradient emanating from the substrate and ending in the bulk [20,21], thus further underscoring the importance of the conformations of the adsorbed chains to

the long-range interfacial effects.

Referring to the conformations of chains in the adsorbed layers, earlier theoretical works predicted that chains adsorbed atop a solid surface adopt conformations in the form of loops, trains and tails [22,23]. Recently, Koga et al. [24,25] experimentally revealed that chains in tightly bound adsorbed layers (also known as flattened layers or bound loop layers [26]) mainly adopted a closely-arranged loop conformation with high-density segment-solid contacts to achieve large enthalpic gains. The concrete picture obtained from its structure now enables the precise design of the adsorbed layers. In this study, we exploit such design to illustrate that the size of loops in the flattened adsorbed layers is a key parameter that controls the propagation of suppressed interfacial dynamics, and accordingly the dynamics, of polymer thin films.

Here, we used a random copolymer of poly(styrene-*ran*-4-hydroxystyrene) P(S-*r*-HS) (see Fig. S1-S3, Table S1 in SM [27] for details of synthesis) to prepare adsorbed layers atop silicon wafers with native oxide layers. Note, that the similar reactivity ratios between S and HS ensure the formation of a statistical copolymer [31,32]. Since HS has a greater affinity to the silicon surface through OH - OH interactions [33], it will preferentially adsorb atop it over the S components in the copolymer, thus providing a means to generate loops in the flattened nanolayers. Control of the loop height of the flattened chains was achieved by changing the mole fraction ( $f_{\text{HS}}$ ) of HS in the copolymer. To obtain adsorbed layers, spin-coated films of P(S-*r*-HS) ( $h = 80 \pm 2$  nm) were annealed at 443 K for 3 hr under vacuum and then solvent-leached using propylene glycol methyl ether acetate (i.e., a good solvent for both PS and PHS) to remove the non-adsorbed chains. The residual layers were dried under vacuum at 393 K for 1 hr and then characterized by ellipsometry, X-ray reflectivity (XRR) and AFM.

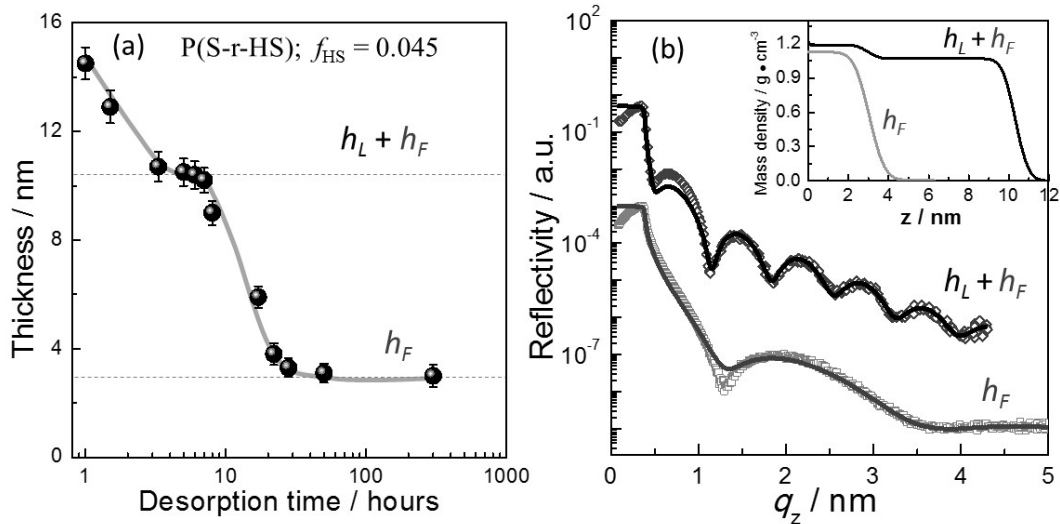


FIG. 1. (a) Thickness of residual layers of P(S-r-HS) as a function of solvent-leaching time. (b) XRR curves of the adsorbed layers consisting of the loosely adsorbed layers ( $h_L$ ) and flattened layers ( $h_F$ ), and only  $h_F$ . The inset of (b) shows density profile of the adsorbed layers.

Figure 1(a) presents the thickness of the residual film of P(S-r-HS) with  $f_{\text{HS}} = 0.045$ , assessed by ellipsometry and XRR, as a function of solvent-leaching time. Notably, two plateaus at thicknesses of 10.4 and 3.0 nm were clearly observed. We note that the two-step desorption behavior has been previously reported and interpreted by Koga et al. [24] and is indicative of the existence of two different architectures within adsorbed layers: inner flattened chains constituted by regularly-arranged loops (i.e., flattened layers), and loosely-adsorbed outer chains with fewer contacts with the substrate. During solvent-leaching between  $3 \text{ hr} < t < 8 \text{ hr}$ , the exposed adsorbed layers consisted of both flattened and loosely adsorbed chains with thickness of  $\sim 10.4 \text{ nm}$ . For solvent leaching  $t > 24 \text{ hr}$ , the second plateau exposed a 3.0 nm thick adsorbed layer consisting only of flattened chains. Results of XRR experiments [see Fig. 1(b)] provided supporting evidence for the existence of

two-layer and single-layer structures for the adsorbed layers with thickness of  $\sim 10.4$  and 3.0 nm, respectively. Combined, the present results suggest that the flattened layer of P(S-r-HS) constituting short loops of adsorbed chains is attainable after extensive solvent-leaching.

Figure 2 shows the thickness of the fattened layers ( $h_F$ ) as a function of  $f_{HS}$ . For  $f_{HS} < 0.024$ ,  $h_F$  increased with increasing  $f_{HS}$ . Between  $0.024 < f_{HS} < 0.14$ ,  $h_F$  decreased with increasing  $f_{HS}$ , and for  $f_{HS} > 0.14$ ,  $h_F$  was independent of the HS content. A quantitative relationship between  $h_F$  and  $f_{HS}$  could be determined based on the proposed nanolayers structure consisting of anchored HS and loop S segments, and is given by Eq. 1 (see Fig. S4 in SM [27] for details):

$$h_F = R \frac{104\sigma}{\rho f_{HS} N_a} \quad (\text{Eq. 1})$$

where  $\sigma$  and  $\rho$  are the number of available anchoring point per unit area and mass density of  $h_F$  ( $\rho = 1.13 \text{ g/cm}^3$  determined by XRR), respectively;  $N_a$  stands for Avogadro's number;  $R$  is a correction parameter reflecting the deviation from the proposed adsorption structure. As shown in Fig. 2, the data were quantitatively fit between  $0.024 < f_{HS} < 0.14$  with  $R = 0.85$  and  $\sigma = 1.1 \text{ nm}^{-2}$ . For  $0.024 < f_{HS}$  and  $f_{HS} > 0.14$ , the deviations in  $h_F$  from the model suggest adsorption of S at the interface and incorporation of HS segments in the loops of the flattened chains, respectively, and thus, bound the  $f_{HS}$  values where the proposed local conformation of loops in the flattened layers, as shown in Fig. 2 are valid. Further support for the proposed structure was obtained by a linear correlation between  $h_F$  and theoretical values of the loop height calculated by geometric analysis; see Fig. S5, S6. AFM images in Fig. S7 revealed smooth and consolidated adsorbed nanolayers atop the substrate, indicating the formation of homogeneous loop structure of flattened chains atop the substrate surface. Taken together, the data presented above demonstrate that the height of loops

in flattened layers can be controlled by altering  $f_{\text{HS}}$ , provided  $0.024 < f_{\text{HS}} < 0.14$ .

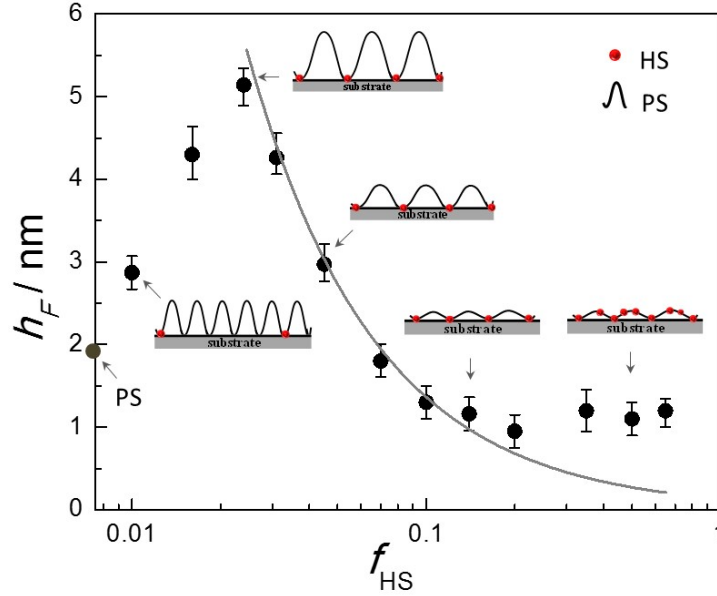


FIG. 2. (a)  $h_F$  as a function of  $f_{\text{HS}}$ . The inset shows the proposed conformation of P(S-r-HS) flattened layers and the brown circle in y axis is the  $h_F$  of PS. The curve is the fit by Eq. 1.

The influence of adsorbed layer chain topology on diffusion in PS thin films was obtained using a multilayer film geometry [34] recently developed to detect gradients of chain mobility near the interface by investigating the diffusion of a fluorinated tracer-labeled polymer. [34] A multilayer film [Inset of Fig. 3(a)] composed of a bottom flattened layer of P(S-r-HS), a variable-thickness middle layer of polystyrene end-capped with 2-perfluorooctylethyl methacrylate (FMA) units (PS<sub>402-ec</sub>-FMA<sub>2</sub>,  $M_w = 43$  kg/mol, PDI = 1.12), and a top layer of PS ( $h_{\text{up}} = 50$  nm,  $M_w = 40$  kg/mol, PDI = 1.08), was fabricated (see section S5 of SM [27] for sample preparations). Upon thermally annealing the multilayer film at 403 K ( $T_g^{\text{bulk}} + 30$  K), the fluorinated chains (PS<sub>402-ec</sub>-FMA<sub>2</sub>) diffuse through the top PS layer, eventually reaching the free surface. The critical time ( $t^*$ ) required for PS<sub>402-ec</sub>-FMA<sub>2</sub> chains to diffuse from the underlying interface to the topmost PS surface, which can be used to determine

effective diffusion coefficients ( $D_{\text{eff}}$ ;  $D_{\text{eff}} = h_{\text{up}}^2/2t^*$ ;  $h_{\text{up}} = 50$  nm) based on Fick's law, were acquired by detecting the onset of water contact angle increment as a function of annealing time due to the enrichment of hydrophobic FMA units at the surface; see Fig 3 (a).

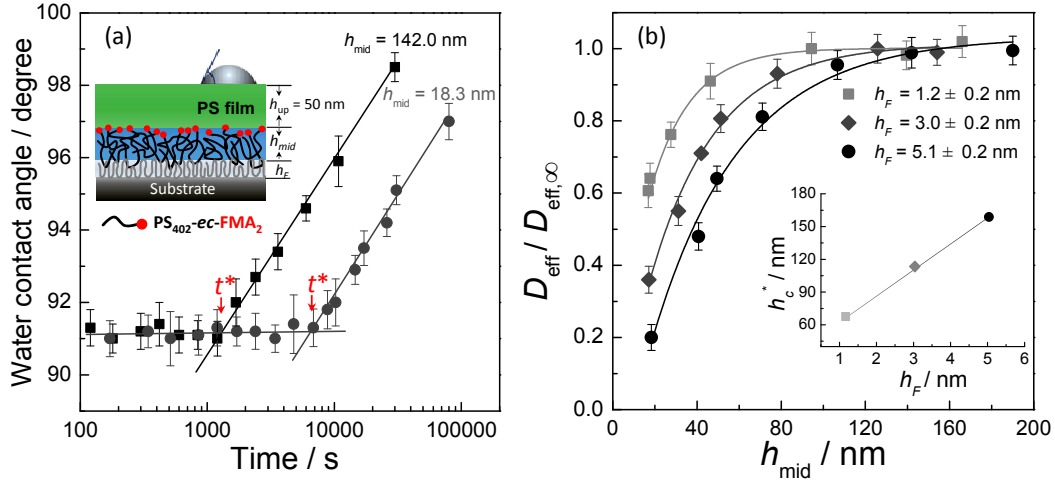


FIG. 3. (a) Water contact angle on top PS surface as a function of annealing time ( $h_{\text{F}} = 5.1$  nm;  $T = 403$  K); (b)  $D_{\text{eff}}/D_{\text{eff},\infty}$  as a function of  $h_{\text{mid}}$  ( $T = 403$  K). Inset of panel (a) and (b) shows the multilayer sample geometry and the relation between the  $h_{\text{c}}^*$  and  $h_{\text{F}}$ , respectively. The straight and curved lines are intended to guide the eye.

Figure 3(b) depicts the normalized diffusion coefficients ( $D_{\text{eff}}/D_{\text{eff},\infty}$ ), where  $D_{\text{eff},\infty}$  is  $D_{\text{eff}}$  when the PS<sub>402-ec-FMA</sub> layer is sufficiently thick that the substrate does not influence mobility of chain at PS//PS<sub>402-ec-FMA</sub> interface, as a function of the PS<sub>402-ec-FMA</sub> layer thickness ( $h_{\text{mid}}$ ). Remarkably, for all films with adsorbed layers having different loop sizes in the flattened layers,  $D_{\text{eff}}/D_{\text{eff},\infty}$  decreased significantly with a reduction in  $h_{\text{mid}}$  below a critical value. Since interfacial effects are known to cause long-range perturbations to molecular mobility and chain diffusion [8,15,20,21,35], the decrease in  $D_{\text{eff}}/D_{\text{eff},\infty}$  is considered to result from interfacial effects exerting a greater influence on mobility as the middle layer thickness is

reduced. In this context, the  $D_{\text{eff}}/D_{\text{eff},\infty}$  vs.  $h_{\text{mid}}$  curves represent the gradient distribution of chain mobility near the interface, and the value of  $h_c^*$ , defined as  $h_{\text{mid}}$  when  $D_{\text{eff}}/D_{\text{eff},\infty} = 0.97$ , were approximated as the critical length scale (or depth) over which a gradient in mobility, originating from interfacial effects at the substrate, could extend within a thin film. Interestingly, the  $h_c^*$  increased markedly with loop height of flattened chains; see insert of Fig. 3(b). At  $h_F = 5.1$  nm, the reduced thin film mobility persisted up to  $\sim 160$  nm (i.e.,  $29R_g$ ) – a distance much larger than that of PS on bare silicon ( $\sim 10R_g$ ) [8, 34]. Our results illustrate that large loops of the flattened chains aid in the propagation of reduced interfacial molecular mobility.

We propose that the loops of the flattened chains provide a structure in which the neighboring unadsorbed chains can penetrate and become entangled, thus propagating suppressed dynamics of the adsorbed chain. To shed light on the changes of such topological interactions, we performed dewetting experiments of PS films (45 nm) atop P(S-r-HS) flattened layers (see experimental details in Section S6 in SM [27]). Since loops of P(S-r-HS) flattened layers have the same chemical structures with the overlaying PS films, dewetting of the PS films from the adsorbed nanolayers is autophobic [36-41] in nature and driven by entropic interaction, and dictated by the extent of chains interpenetration. Upon annealing at 423 K, the PS films readily dewet the adsorbed layers with  $h_F \leq 4.2$  nm; however, the films remained stable on the adsorbed layers with  $h_F = 5.1$  nm; see Fig 4(a) inset, consistent with the ‘wet’ condition with strong interpenetration [39]. The relationship between the degree of interpenetration and loop height of the flattened chains was assessed by probing the interface slippage. Polymers can better slip at the interface with less interpenetration, while stronger interpenetration, associated with large interfacial friction, usually cause less slippage with a smaller slip length ( $b$ ). [40-42] The interfacial slip length ( $b$ ); ( $b \sim$

$1/k$ ,  $k$ : interfacial friction coefficients [40-42]) — a parameter characterizing the degree of “slippiness” — of PS on the various adsorbed layers was evaluated by examining the dewetting dynamics (see Section 6 of SM [27] for the calculations of  $b$ ). It is evident that the slip length tends to decrease (indicating less slippiness) with increasing loop height of the flattened chains; see Fig. 4 (a), thus indicating the increased interfacial friction due to the formation of stronger interpenetrations and entanglements between loops in flattened layers and free chains in the matrix.

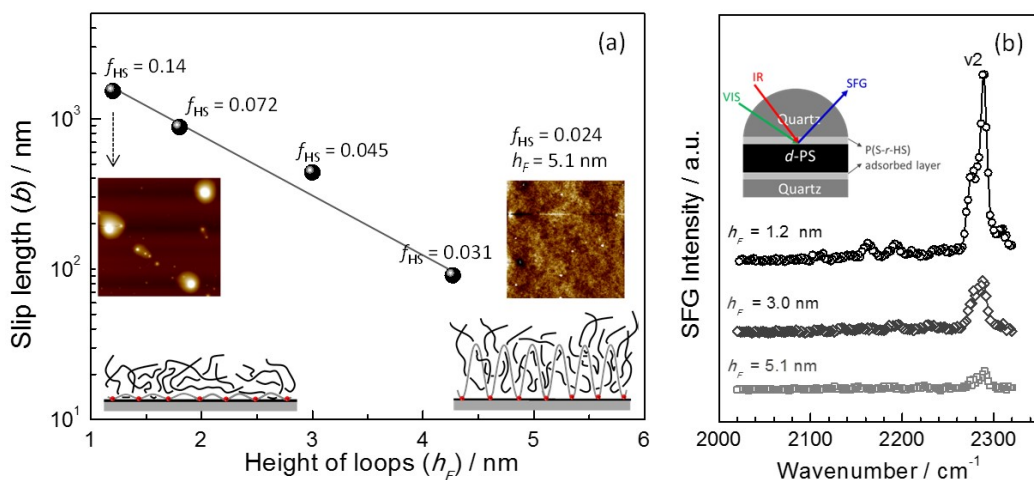


FIG. 4. (a) Slip length and AFM images of PS films on the adsorbed layers; (b) SFG spectra from the polymer-polymer interfaces between the adsorbed and the non-adsorbed chains. Insets of panel (a) and (b) illustrate the differences in interpenetration and entanglements formed between the adsorbed and neighboring free chains at low and high  $h_F$ , and sample geometry for SFG measurements, respectively. The size of AFM images in (a) is  $32 \times 32 \mu\text{m}$ .

The interface of the flattened adsorbed layers was directly probed by a sum frequency generational spectroscopy (SFG). A sandwiched sample geometry; shown in the inset of Fig. 4(b), (see sample preparations in Section 7 of SM [27]) was used to acquire SFG signals from the interface of a deuterated PS film ( $d$ -PS) and underlying P(S-r-HS) adsorbed layers. When the loop height of flattened chains was small (e.g.,  $h_F = 1.2$  nm), strong signals in C-D vibrational region from phenyl ring of  $d$ -PS (i.e.,

$\nu_2$  at  $2280\text{ cm}^{-1}$  [43]) appeared in the SFG spectra; see Fig. 4(b). However, the peak intensities decreased upon increasing height of the loops in the flattened adsorbed layers. Since SFG signal is generated at an interface where the symmetry is broken and molecules are ordered [44], it could be reasonably inferred that a sharp and contrasting interface normally generates strong SFG signals, however a gradient and diffusive interface results in weak signals because of the loss of the molecular ordering at the interface [45]. Therefore, the SFG results also evidenced the notion that the flexible loops formed by the flattened chains facilitated the interpenetration and entanglements with the free chains in matrix, and the strength of such topological interaction increased with increasing the loop height.

Taken together, results presented above, demonstrate that the ability to tune the propagation of suppressed dynamics by a new parameter, i.e., the loop height of the flattened nanolayers, is essentially correlated to the topological interactions, which we regard to result from interpenetration and entanglement between the chains anchored to the surface and those without direct contact with substrate. The increased topological interaction strengthen the degree of motional coupling of chains, resulting in an increase in the distance of hindrance to interfacial dynamics with increasing loop height [Fig. 3b].

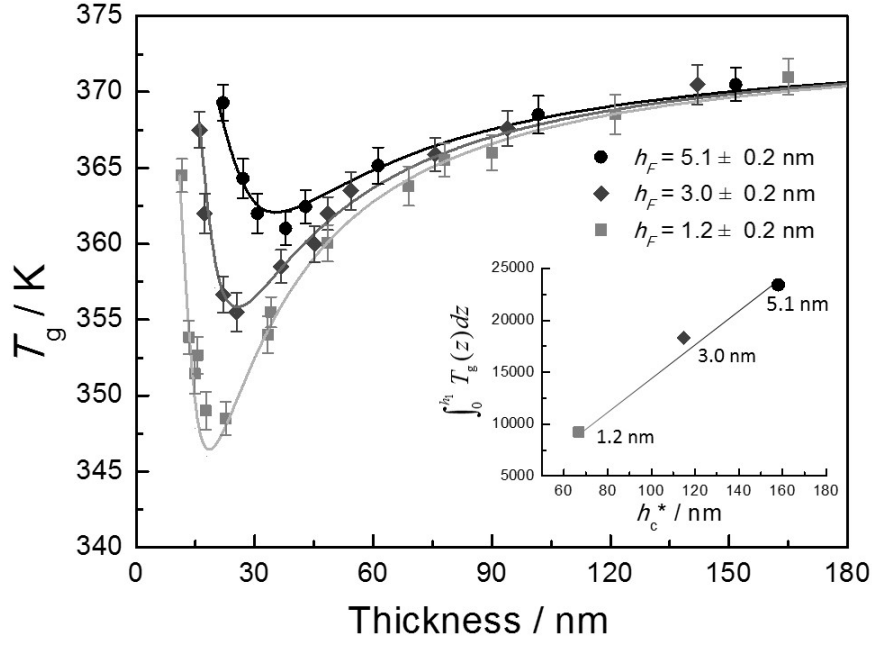


FIG 5.  $T_g$  of PS films supported by the adsorbed layers as functions of the film thickness. The inset displays the linear correlations between  $\int_0^{h_c} T_g(z) dz$  and  $h_c^*$ . The solid curves represent the best fitting of the  $T_g$  using the three-layer model (Eq.2) to extract  $\int_0^{h_c} T_g(z) dz$ .

Finally, we show how the differences in adsorbed nanolayer topology can be used to tune the  $T_g$ -confinement behavior of the PS films, i.e., a demonstration of exploiting confinement for property manipulation. As shown in Fig. 5,  $T_g$  of thin PS films on the P(S-r-HS) adsorbed layer surface, as measured by ellipsometry, firstly decrease due to free surface effects [46,47] and then increase because of the dominance of interfacial effect [46,47] with reducing the film thickness. The threshold film thickness for the observed increase in  $T_g$  for PS thin film is greater when placed atop adsorbed flattened nanolayers with larger loops, that is 18, 26 and 33 nm for PS film on adsorbed layer with  $h_F = 1.2, 3.0$  and  $5.1$  nm, respectively. We note that the non-monotonic change in  $T_g$ , arising from the counteraction between interface and free surface effects, was previous observed for PS-COOH on SiOx, but the increase in

$T_g$  occurred at much smaller thicknesses (i.e.,  $< 10$  nm) [48,49]. The larger threshold values indicate that the loop structures of the P(S-r-HS) flattened chains which aid the propagation of suppressed interfacial dynamics amplify the influence of interfacial effect. The contribution of interfacial effects on  $T_g$  of PS films was extracted by fitting  $T_g(h)$  vs. thickness curves; see Fig. 5 using a three-layers model containing a surface mobile layer, a bulk region and an interfacial layers [47,50,51].

$$T_g(h) = \frac{h - h_1}{h} T_g^{\text{bulk}} \left[ 1 - \left( \frac{\gamma}{h} \right)^\delta \right] + \frac{\int_0^{h_1} T_g(z) dz}{h} \quad (2)$$

The first term in Eq. 2 reflects the effects of a mobile free surface, in which  $\gamma$  and  $\delta$  are surface-related parameters ( $\gamma = 3.2 \pm 0.6$  nm,  $\delta = 1.8 \pm 0.2$  for PS) [50,51];  $h_1$  is thickness of the interfacial layers. The second term accounts for the contribution of suppressed interfacial dynamics, in which  $T_g(z)$  is a function describing the depth distribution of local  $T_g$ , and the integration ( $\int_0^{h_1} T_g(z) dz$ ) is the sum of  $T_g(z)$  of all the sub-layers with different distances from the adsorbed layers. It was shown that the integral term increases with increase the loop height of the flattened chains, as shown in inset of Fig. 5. Moreover,  $\int_0^{h_1} T_g(z) dz$  correlates linearly with the distance at which the substrate affects polymer mobility ( $h_c^*$ ); see Fig. 5. Figure 5 also illustrated that both  $h_c^*$  and  $T_g$  of the PS thin film increased with the thickness of the flattened layer. This behavior is qualitatively consistent with that reported in homopolymer [12,13], in which a correlation between adsorbed amount and materials properties was identified, and therefore further support the claim that the chain adsorption governs the equilibrium and non-equilibrium dynamics of confined polymers.

This letter points to new physics in understanding interfacial effects on relaxation dynamics of the nanoconfined polymers: the local conformation of chains

adsorbed atop solid surfaces plays a vital role on the propagation of suppressed dynamics induced by interacting substrates, by altering topological interactions of chains at the polymer-polymer interface with the adsorbed structure of chains closest to the substrate. The flattened adsorbed chains with larger loops are highly efficient in propagating suppressed interfacial dynamics because of their ease in forming strong topological constrains with free chains, giving rise to interfacial effects which can be propagated far away from the substrate. Results of this study enable an opportunity to tune the length scale that interfacial effects propagate by the rationalized optimization of local conformation, and more specifically size of loops, of the adsorbed flattened chains on solid surface, and thus have strong implications on reinforced polymer nanocomposites, where the filler/polymer interface is believed to be important.

#### **Acknowledgements:**

We acknowledge financial support from Natural Science Foundation of China (Grants 21504081 and 21674100) and the National Science Foundation (NSF) Materials Research Science and Engineering Center Program through the Princeton Center for Complex Materials (DMR-1420541). R.D.P. acknowledges the NSF through CBET – 1706012.

\*To whom all correspondence should be addressed.

wxinping@zstu.edu.cn.

†To whom all correspondence should be addressed.

rpriestl@princeton.edu.

#### **Reference:**

- [1] M. Alcoutlabi, and G. B. McKenna, Effects of confinement on material behaviour at the nanometre size scale, *J. Phys.: Condens. Matter* **17**, R461 (2005).
- [2] M. D. Ediger, and J. A. Forrest, Dynamics near free surfaces and the glass transition in thin polymer films: a view to the future, *Macromolecules* **47**, 471 (2014).
- [3] S. Napolitano, E. Glynos, and N. B. Tito, Glass transition of polymers in bulk, confined geometries, and near interfaces, *Rep. Prog. Phys.* **80**, 036602 (2017).
- [4] R. D. Priestley, C. J. Ellison, L. J. Broadbelt, and J. M. Torkelson, Structural relaxation of polymer glasses at surfaces, interfaces, and in between, *Science* **309**, 456 (2005).
- [5] Z. Yang, Y. Fujii, F. K. Lee, C-H. Lam, and O. K. C. Tsui. Glass transition dynamics and surface layer mobility in unentangled polystyrene films, *Science* **328**, 1676 (2010).
- [6] C. J. Ellison, and J. M. Torkelson, The distribution of glass-transition temperatures in nanoscopically confined glass formers, *Nature Mater.* **2**, 695 (2003).
- [7] A. Papon, H. Montes, M. Hanafi, F. Lequeux, L. Guy, and K. Saalwachter, Glass-transition temperature gradient in nano-composites: evidence from nuclear magnetic resonance and differential scanning calorimetry, *Phys. Rev. Lett.* **108**, 065702 (2012).
- [8] X. Zheng, M. H. Rafailovich, J. Sokolov, Y. Strzhemechny, S. A. Schwarz, B. B. Sauer, and M. Rubinstein, Long-range effects on polymer diffusion induced by a bounding interface, *Phys. Rev. Lett.* **79**, 241 (1997).
- [9] D. Long, and F. Lequeux, Heterogeneous dynamics at the glass transition in van der Waals liquids, in the bulk and in thin films, *Eur. Phys. J. E* **4**, 371 (2001).
- [10] A. Papon, K. Saalwächter, K. Schäler, L. Guy, F. Lequeux, and H. Montes, Low-field NMR investigations of nanocomposites: polymer dynamics and network

effects, *Macromolecules* **44**, 913(2011).

[11] S. Napolitano and M. Wübbenhorst, The lifetime of the deviations from bulk behavior in polymers confined at the nanoscale, *Nature Commun.* **2**, 260 (2011).

[12] A. Panagopoulou and S. Napolitano, Irreversible adsorption governs the equilibration of thin polymer films, *Phys. Rev. Lett.* **119**, 097801 (2017).

[13] N. G. Perez-de-Eulate, M. Sferrazza, D. Cangialosi, and S. Napolitano, Irreversible adsorption erases the free surface effect on the  $T_g$  of supported films of poly(4-tert-butylstyrene), *ACS Macro Lett.* **6**, 354 (2017).

[14] D. N. Simavilla, W. Huang, C. Housmans, M. Sferrazza, and S. Napolitano, Taming the strength of interfacial interactions via nanoconfinement, *ACS Cent. Sci.* **4**, 755 (2018).

[15] T. Koga, N. Jiang, P. Gin, M. K. Endoh, S. Narayanan, L. B. Lurio, and S. K. Sinha, Impact of an irreversibly adsorbed layer on local viscosity of nanoconfined polymer melts, *Phys. Rev. Lett.* **107**, 225901 (2011).

[16] J. Xu, Z. Liu, Y. Lan, B. Zuo, X. Wang, J. Yang, W. Zhang, and W. Hu, Mobility gradient of poly(ethylene terephthalate) chains near a substrate scaled by the thickness of the adsorbed layer, *Macromolecules* **50**, 6804 (2017).

[17] S. Sun, H. Xu, J. Han, Y. Zhu, B. Zuo, X. Wang, and W. Zhang, The architecture of the adsorbed layer at the substrate interface determines the glass transition of supported ultrathin polystyrene films, *Soft Matter* **12**, 8348 (2016).

[18] B. Zuo, J. Xu, S. Sun, Y. Liu, J. Yang, L. Zhang, and X. Wang, Stepwise crystallization and the layered distribution in crystallization kinetics of ultra-thin poly(ethylene terephthalate) film, *J. Chem. Phys.* **144**, 234902 (2016).

[19] M. J. Burroughs, S. Napolitano, D. Cangialosi, and R. D. Priestley. Direct measurement of glass transition temperature in exposed and buried adsorbed polymer

- nanolayers, *Macromolecules* **49**, 4647-4655(2016).
- [20] N. Jiang, L. Sendogdular, X. Di, M. Sen, P. Gin, M. K. Endoh, T. Koga, B. Akgun, M. Dimitriou, and S. Satija, Effect of CO<sub>2</sub> on a mobility gradient of polymer chains near an impenetrable solid, *Macromolecules* **48**, 1795 (2015).
- [21] M. Krutyeva, A. Wischnewski, M. Monkenbusch, L. Willner, J. Maiz, C. Mijangos, A. Arbe, J. Colmenero, A. Radulescu, O. Holderer, M. Ohl, and D. Richter, Effect of nanoconfinement on polymer dynamics: surface layers and interphases, *Phys. Rev. Lett.* **110**, 108303 (2013).
- [22] K. Motomura, and R. Matuura. Conformation of adsorbed polymeric chain. II, *J. Chem. Phys.* **50**, 1281 (1969).
- [23] G. J. Fleer, M.A. Cohen-Stuart, J. M. H. M. Scheutjens, T. Cosgrove, and B. Vincent, *Polymers at Interfaces* (Chapman Hall, London, 1993).
- [24] P. Gin, N. Jiang, C. Liang, T. Taniguchi, B. Akgun, S. K. Satija, M. K. Endoh, and T. Koga, Revealed architectures of adsorbed polymer chains at solid-polymer melt interfaces, *Phys. Rev. Lett.* **109**, 265501 (2012).
- [25] N. Jiang, J. Shang, X. Di, M. K. Endoh, and T. Koga, Formation mechanism of high-density, flattened polymer nanolayers adsorbed on planar solids, *Macromolecules* **47**, 2682 (2014).
- [26] S. Cheng, A. P. Holt, H. Wang, F. Fan, V. Bocharova, H. Martin, T. Etampawala, B. T. White, T. Saito, N-G. Kang, M. D. Dadmun, J. W. Mays, and A. P. Sokolov, Unexpected molecular weight effect in polymer nanocomposites, *Phys. Rev. Lett.* **116**, 038302 (2016).
- [27] See Supplemental Material for (1) synthesis of the P(S-r-HS) copolymers; (2) deducing the quantitative relation between  $h_F$  and  $f_{HS}$ ; (3) estimation of  $h_{Theo}$ ; (4) AFM images of the P(S-r-HS) adsorbed layers; (5) preparation of the multilayer films used for diffusion measurement; (6) determination of the slip length; (7) basic

principle and experimental details for the SFG measurements, which include Refs. [28-30]

[28] F. Brochard-Wyart, P.-G. de Gennes, H. Hervert, and C. Redon, Wetting and slippage of polymer melts on semi-ideal surfaces, *Langmuir* **10**, 1566 (1994).

[29] F. Vidal, and A. Tadjeddine, Sum-frequency generation spectroscopy of interfaces. *Rep. Prog. Phys.* **68**, 1095 (2005).

[30] B. Zuo, M. Inutsuka, D. Kawaguchi, X. Wang, and K. Tanaka, Conformational relaxation of poly(styrene-co-butadiene) chains at substrate interface in spin-coated and solvent-cast films, *Macromolecules* **51**, 2180 (2018).

[31] M. M. Vaidya, K. Levon, and E. L. I. M. Pearce, Miscibility of poly ( $\epsilon$ -caprolactone), a semicrystalline polymer, with amorphous poly (styrene-4-hydroxystyrene) copolymers, *J. Polym. Sci. Polym. Phys.* **33**, 2093 (1995).

[32] K. J. Zhu, S. F. Chen, T. Ho, E. M. Pearce, and T. K. Kwei, Miscibility of copolymer blends, *Macromolecules* **23**, 150 (1990).

[33] R. S. Tate, D. S. Fryer, S. Pasqualini, M. F. Montague, J. J. de Pablo, and P. F. Nealey, Extraordinary elevation of the glass transition temperature of thin polymer films grafted to silicon oxide substrates, *J. Chem. Phys.* **115**, 9982 (2001).

[34] J. Xu, Y. Zhang, H. Zhou, Y. Hong, B. Zuo, X. Wang, and L. Zhang, Probing the utmost distance of polymer dynamics suppression by a substrate by investigating the diffusion of fluorinated tracer-labeled polymer chains, *Macromolecules* **50**, 5905 (2017).

[35] R. Inoue, M. Nakamura, K. Matsui, T. Kanaya, K. Nishida, and M. Hino, Distribution of glass transition temperature in multilayered poly(methyl methacrylate) thin film supported on a Si substrate as studied by neutron reflectivity. *Phys. Rev. E* **88**, 032601 (2013).

[36] G. Reiter, J. Schultz, P. Auroy and L. Auvray, Improving adhesion via connector polymers to stabilize non-wetting liquid films. *Europhys. Lett.* **33**, 29 (1996).

[37] L. Leibler, and A. Mourran, Wetting on grafted polymer films, *MRS Bull.* **22**, 33 (1997).

- [38] P. G. Ferreira, A. Ajdari, and L. Leibler, Scaling law for entropic effects at interfaces between grafted layers and polymer melts, *Macromolecules* **31**, 3994 (1998).
- [39] H. Oh, and P. F. Green, Polymer chain dynamics and glass transition in athermal polymer/nanoparticle mixtures, *Nature Mater.* **8**, 139 (2009).
- [40] G. Reiter and R. Khanna, Real-Time determination of the slippage length in autophobic polymer dewetting, *Phys. Rev. Lett.* **85**, 2753 (2000).
- [41] G. Reiter, and R. Khanna, Kinetics of autophobic dewetting of polymer films, *Langmuir* **16**, 6351 (2000).
- [42] R. Fetzer, M. Rauscher, A. Munch, B. A. Wagner, and K. Jacobs, Slip-controlled thin-film dynamics, *Europhys. Lett.* **75**, 638(2006).
- [43] Y. Hong, Y. Li, F. Wang, B. Zuo, X. Wang, L. Zhang, D. Kawaguchi, and K. Tanaka, Enhanced thermal stability of polystyrene by interfacial noncovalent interactions, *Macromolecules* **51**, 5620 (2018).
- [44] Y. R. Shen, Surface properties probed by second-harmonic and sum-frequency generation, *Nature* **337**, 519 (1989).
- [45] J. Wang, C. L. Loch, D. Ahn, and Z. Chen, Demonstrating the feasibility of monitoring the molecular-level structures of moving polymer/silane interfaces during silane diffusion using SFG, *J. Am. Chem. Soc.* **126**, 1174 (2004).
- [46] M. Campoy-Quiles, M. Sims, P. G. Etchegoin, and D. D. C. Bradley, Thickness-dependent thermal transition temperatures in thin conjugated polymer films, *Macromolecules* **39**, 7673 (2006).
- [47] D. Liu, R. O. Orozco, and T. Wang, Deviations of the glass transition temperature in amorphous conjugated polymer thin films, *Phys. Rev. E* **88**, 022601 (2013).
- [48] J. L. Keddie, and R. A. L. Jones. Glass transition behavior in ultra-thin

polystyrene films, *Isr. J. Chem.* **35**, 21 (1995).

[49] J. A. Forrest and J. Mattsson, Reductions of the glass transition temperature in thin polymer films: probing the length scale of cooperative dynamics, *Phys. Rev. E* **61**, R53(R) (2000).

[50] J. L. Keddie, R. A. L. Jones, and R. A. Cory, Size-dependent depression of the glass transition temperature in polymer films, *Europhys. Lett.* **27**, 59 (1994).

[51] J. L. Keddie, R. A. L. Jones, and R. A. Cory, Interface and surface effects on the glass-transition temperature in thin polymer films, *Faraday Discuss.* **98**, 219 (1994).